1986

Noise Reduction of Rolling Piston Type Rotary Compressor

S. Kawaguchi

T. Yamamoto

T. Hirahara

Ohinata

K. Morinushi

NOISE REDUCTION OF ROLLING PISTON TYPE ROTARY COMPRESSOR

Susumu Kawaguchi[1], Ken Morinushi[2], Takashi Yamamoto[1], Takuho Hirahara[1] and Okinobu Ohinata[1]

[1] Shizuoka Works, Mitsubishi Electric Corporation Shizuoka,Japan
[2] Central Research Laboratory, Mitsubishi Electric Corporation Amagasaki, Hyogo, Japan

ABSTRACT

This paper refers to the noise reduction of the rolling piston type rotary compressor. In general, as the rolling piston increases its speed under the high compression ratio condition, the noise level increases steeply. We resume that this happens because a certain shock wave is produced in the compression space. Then we could simulate the phenomenon by the numerical analysis (CACE method) of unsteady one-dimensional flow. As the countermeasure of the shock wave, we formed escape grooves in a wall of the discharge port at an upstream side of the crank angle from the discharge port, and then we could reduce the noise level of the rolling piston type rotary compressor.

INTRODUCTION

The rolling piston type rotary compressor has been widely used for air conditioners and refregerators. In recent years, in regard to the development of variable-speed rotary compressors, the noise reduction has become a very important problem. The noise reduction of rotary compressors has been examined by various authors from different points of view. Generally, the following facts have been considered as main causes of the noise.[(1)(2)(3)]

1) The jet flow which is produced when the discharge gas is let out of cylinder chamber
2) The vibration caused by the collision and the sliding between compressor parts
3) The electromagnetic force

In some test conditions of compressors, a phenomenon occurred. It could not be explained well by the above causes. It is the phenomenon that the noise and the vibration increase before the discharge valve is forced to open, and before the discharge gas is let out of the cylinder chamber. After having investigated the vibration timing and the pressure pulsation in the cylinder compression space, we could make sure that the shock wave occurred in the cylinder compression space and that the high frequency pressure pulsation which was caused by the shock wave excited compressor parts. As a result of the countermeasure for the shock wave, we could reduce the noise level of the compressor.

ANALYSIS OF NOISE AND VIBRATION

Test Compressors And Test Procedures

Fig.1 and Fig.2 show the constructions of the test compressors. Fig.1 shows the construction of the rolling piston type test compressor (open type one), and we call this one MODEL A. MODEL A is driven by motors or engines. The stroke volume of MODEL A is 79.8(cc/rev). Table 1 shows the test conditions of MODEL A. Fig.2 shows the construction of the hermetic test compressor, and we call this one MODEL B. MODEL B is used in air coditioners and has the following specifications.

Stroke volume : 39.0 (cc/rev)
Nominal output : 1700 (w)

And MODEL B was tested by the conditions of table 2.

The noise was measured in an anechoic room. In the case of MODEL A, the noise level was measured at a distance of 1 meter from the compressor shell surface. In the case of MODEL B, it was measured at a distance of 50 cm from the shell surface. These tests can measure the noise and the vibration of the compresors. At the same time, it is possible to measure the crank angle, the valve displacement and the pressure of the compression space in the cylinder. And signals from the sensors were measured with various B&K instruments and the data were analyzed by FFT analyzer (HP5451C).

Test Results And Discussions

Fig.3 shows the test results of MODEL A on the A-3 condition. From Fig.3 we found that there was the high frequency pressure pulsation on the pressure of the compression space in the cylinder, and that

the noise and the vibration increase gradually before the discharge valve was forced to open, except that the noise and the vibration occurred while the discharge valve was open.
Fig.4 and Fig.5 show the test results of MODEL B on the B-4 and B-5 conditions. Through all the tests (table 2) we found the high frequency pressure pulsation like MODEL A. We also found that the high frequency pressure pulsation increased as the piston increased its speed and that the vibration increased owing to the high frequency pressure pulsation.

Next, we examine how the high frequency pressure pulsation occurs. This pressure pulsation increases under high revolutionary speed and high compression ratio conditions. We presume as follows, the reason of the above phenomena is because the shock wave is produced in the compression space. And the shock wave is caused by the fact that the high pressure gas and the low pressure gas communicate instantaneously, when the piston is about to pass by the discharge ports.(see Fig.6) This phenomenon is the same one as the shock wave arises when a diaphragm which divides a shock tube into the high pressure side and the low pressure side is broken. This pressure pulsation vibrates the cylinder, the piston and the other parts of compressors. This pulsation increases the level of the noise and the vibration.

NUMERICAL ANALYSIS

We make one-dimensional model (Fig.7) to simulate the shock wave which occurs in the compression space of the cylinder. We explain this model as follows. The compression space is divided by a diaphragm into a high pressure side (, which has the smaller space) and a low pressure side (, which has the larger space). And when the diaphragm is instantaneously broken, the high pressure gas begins to flow out to the low pressure side. At the same time, the piston moves from the right to the left with the velocity :$u_p(t)$ (Fig.7-A) and begins to compress the gas in the compression space.

To explain simply the compressible gas flow in the compression space, we constructed mathematical model as unsteady one-dimensional flow. This model is governed by the following equations.

Continuity equation

$$\frac{\partial \rho}{\partial t} + \frac{\partial}{\partial x}(\rho u) = 0$$

Momentum equation

$$\frac{\partial}{\partial t}(\rho u) + \frac{\partial}{\partial x}(\rho u^2 + p) = 0$$

Energy equation

$$\frac{\partial}{\partial t}(\rho e_s) + \frac{\partial}{\partial x}\{ \rho u (e_s + p/\rho) \} = 0$$

Equation of heat state

$$p/\rho = \frac{\gamma - 1}{\gamma}(h_s - 0.5 u^2)$$

where,

ρ = density of gas
u = velocity of gas
p = pressure of gas
$e_s = e + 0.5u^2$ internal energy of stagnation point
e = internal energy
$h_s = e_s + p/\rho$, enthalpy of stagnation point
$\gamma = c_p / c_v$, ration of specific heats

we analyzed these equations of unsteady one-dimensional flow with the numerical analysis method-CACE (Compressible Advanced, Continuous-fluid, Eulerian).(4)

Fig.7-b illustrates the corresponding distribution of the piston velocity $u_p(t)$. Fig.7-c illustrates the mesh division of CACE method, and the definition of ρ, p, h_s and ρu. Fig.8 and Fig.9 show the results of this numerical calculation on the A-3 condition. Calculating conditions are as follows.

IMAX = 501		: the number of mesh
Id = 4		: the point of diaphragm
L = 150 mm		: cylinder length
$\Delta X = 0.3\times10^{-3}$	m	: space mesh
$\Delta T = 0.8\times10^{-6}$	sec	: time mesh
γ = 1.141		: ration of specific heats
Pd = 1.52 MPa		: dischage pressure
Ps = 0.16 MPa		: suction pressure

Fig.8 shows the simulation result of the pressure pulsation at the point where there was a diaphragm, and we find as follows. The high frequency pressure pulsation appears. During a compression process, the cycle time of the high frequency pulsation becomes gradually shorter and the pulsation is gradually amplified. Fig.9 shows the propagation of the shock wave at each time, and we find as follows. At first the shock wave is propagated from the left to the right owing to the break of the diaphragm, and then

the shock wave is rebounded by the piston and is propagated to the left. Because of the above facts, it can be said that this calculated pressure pulsation is similar to the one of test results. And we found that the high pressure gas and the low pressure gas should be made to communicate little by little.

TEST RESULTS OF THE IMPROVED MODEL

Fig.10 shows the important cylinder part of improved model. We formed escape grooves in the wall surface of the cylinder at the upstream side of the crank angle from the discharge ports.

We made several tests in changing width, depth and curvature of the escape grooves, and then we obtained interesting results.
Fig.11 shows the noise pattern of each specification of escape grooves. From this figure, we find that these specifications are A > B > C > D, in order of noise level, and we could make sure that the obvious relation was observed between the noise level of the rolling piston type rotary commpressor and the form of escape grooves.
Fig.12 shows the noise, the vibration, the pressure pulsation, and the valve displacement of improved MODEL A'. Making a comparison between Fig.3 and Fig. 12, we get to know that the escape groove is effective as regards the noise reduction.
Fig.13 shows the pressure pulsation power spectra before and after the escape grooves are formed. We find that the pressure pulsation is damped over a broad frequency band, particularly in the region from 1,000 to 3,000 Hz.
Fig.14 and Fig.15 show the pressure pulsation and the vibration of improved MODEL B'. We find that the high frequency pressure pulsation and the vibration of improved MODEL B'are smaller than those of old MODEL B.
Fig.16 and Fig.17 show the noise level of MODEL A, MODEL A', MODEL B, and MODEL B'on each condition. From these figures we find that the escape grooves are very effective in the noise reduction especially under the high revolutionary speed conditions and the high compression ratio conditions.

CONCLUSION

1. We made sure that the shock wave occured in the compression space of cylinder and that this shock wave was one of the main causes of the rolling piston type rotary compressor.

2. We could simulate this shock wave with the analysis (CACE method) of unsteady one-dimensional flow.

3. As we formed escape grooves in a wall of discharge ports, we could reduce the high pressure pulsation which is caused by the shock wave. As a result, we could reduce the noise level into about 10 dBA on the A-3 condition of MODEL A and into about 5 dBA on the B-4 condition of MODEL B.

REFERENCES

(1) H. Tanaka et al.,"Noise and Efficiency of Rolling Piston Type Refrigeration Compressor for Household Refrigerator and Freezer" Proc.1980 Purdue Comp. Tech. Conf.

(2) K. Asami et al.,"Improvements of Noise and Efficiency of Rolling Piston Type Refrigeration Compressor for Household Refrigerator and Freezer" Proc. 1982 Purdue Comp. Tech. Conf.

(3) K. Sano et al.,"Analysis of Hermetic Rolling Piston Type Compressor Noise,and Countermeasures" Proc. 1984 Int. Comp. Eng. Conf. at Purdue

(4) C.W.Stewart et al.,"A Eulerian Computation Method for Fluid Flows with Large Density Gradients at All Speeds" Nucl. Sci. Eng. 64 (1977)

Table 1 Test conditions for MODEL A

Refrigerant : R-12

Revolution (rpm)	Pd (MPa)	Ps (MPa)	Ts (°C)	Condition number
1800	1.52	0.31	10	A-1
2700	1.52	0.22	0	A-2
3600	1.52	0.16	-8	A-3
5400	1.52	0.16	-8	A-4

Table 2 Test conditions for MODEL B

Refrigerant : R-22

Revolution (rpm)	Pd (MPa)	Ps (MPa)	Ts (°C)	Condition number
3400	2.03	0.58	15	B-1
	2.03	0.30	-5	B-2
	2.03	0.20	-15	B-3
5100	2.03	0.58	15	B-4
	2.03	0.30	-5	B-5
	2.03	0.20	-15	B-6

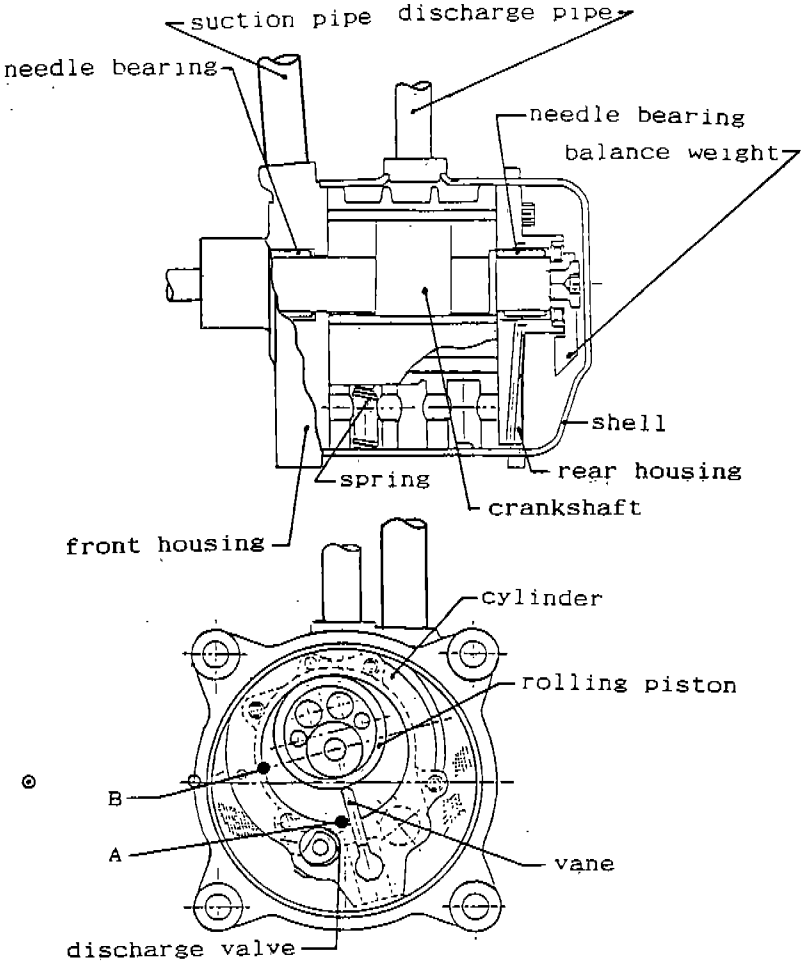

● A,B: pressure transducer(Kistler type 601A)
point A = crank angle 355°
point B = crank angle 270°

○ : accelerometer
B&K type 4344

⊙ : microphone
B&K type 4145

Fig.1 Sectional view of MODEL A

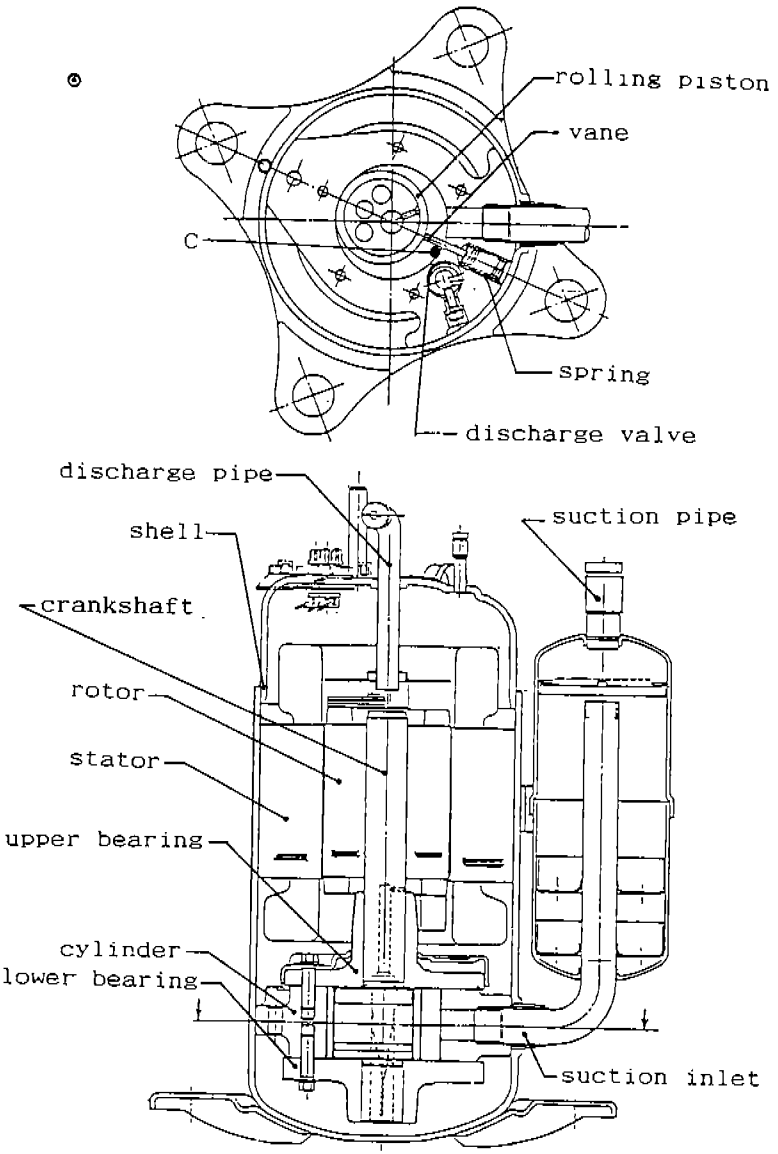

● C: pressure transducer(Kistler type 601A)
point C = crank angle 355°
○ : accelerometer
B&K type 4344
⊙ : microphone
B&K type 4145

Fig.2 Sectional view of MODEL B

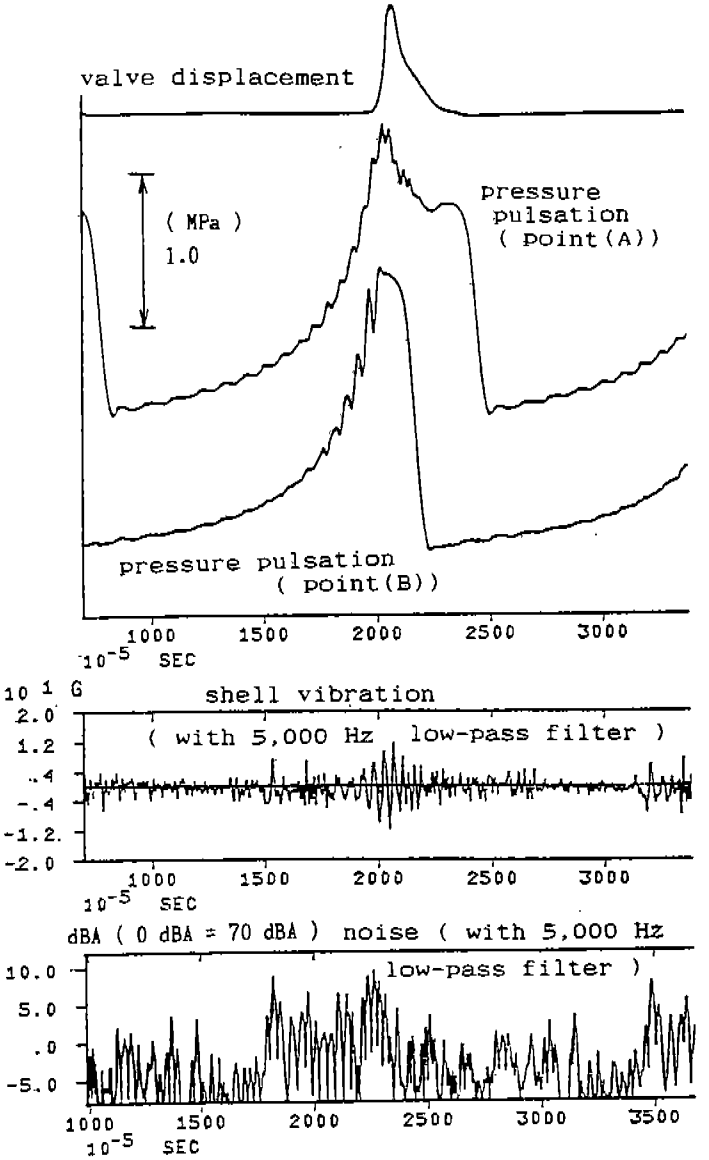

Fig.3 Test data of MODEL A on the A-3 condition

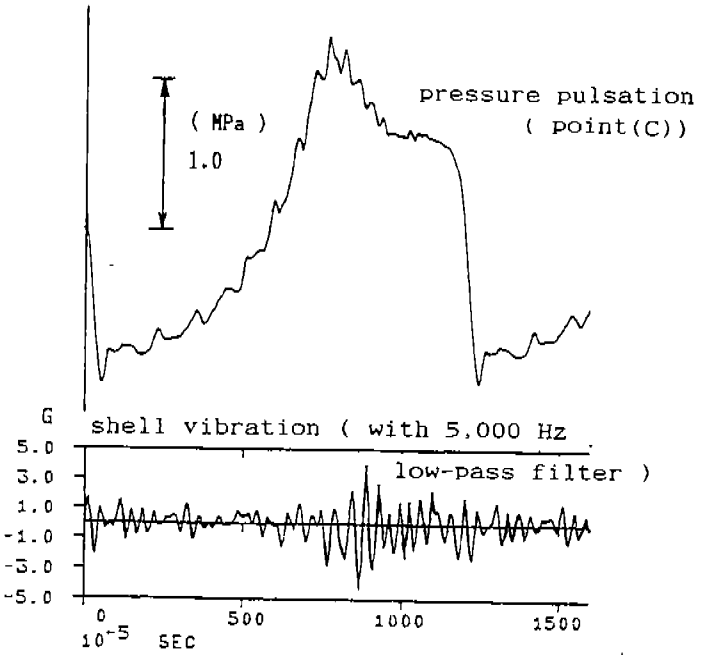

Fig.4 Test data of MODEL B on the B-4 condition

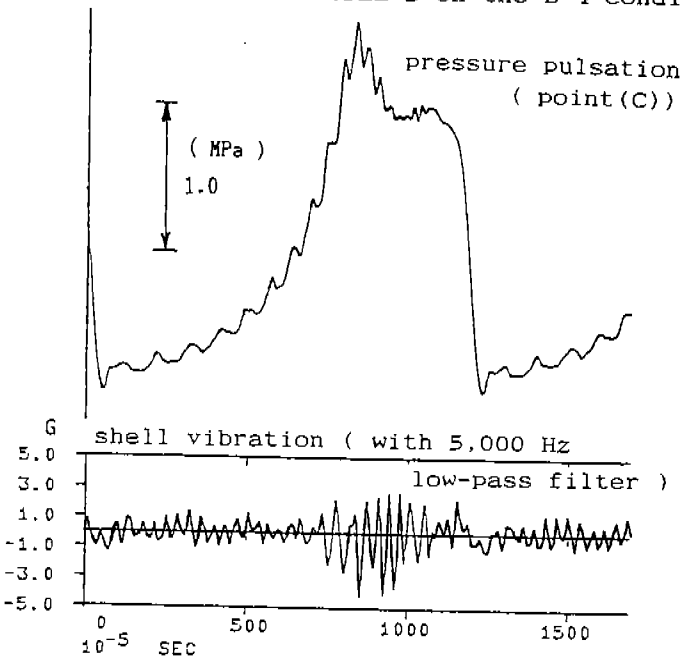

Fig.5 Test data of MODEL B on the B-5 condition

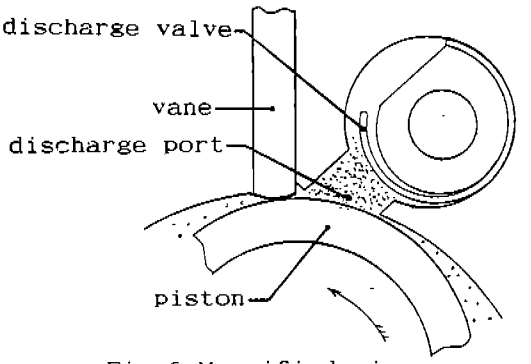

Fig.6 Magnified view
around discharge port

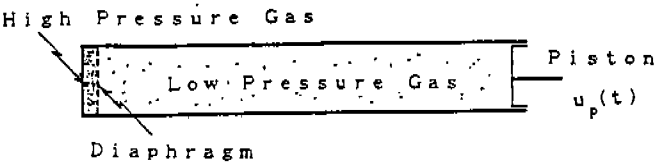

(a) One-dimensional model

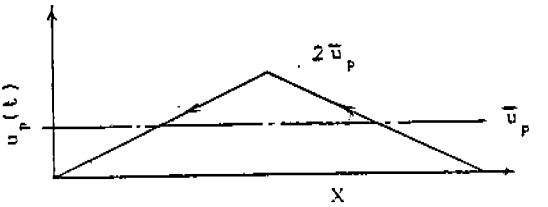

(b) Piston velocity

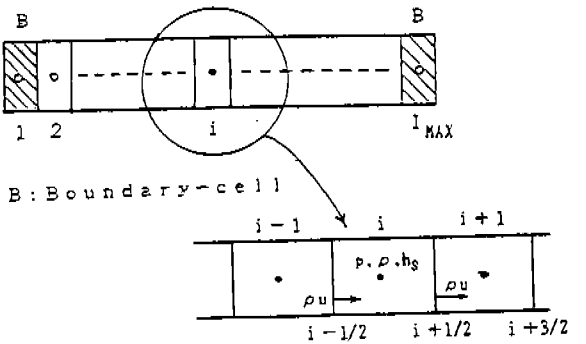

(c) Mesh division of CACE method

Fig.7 One-dimensional simulation model

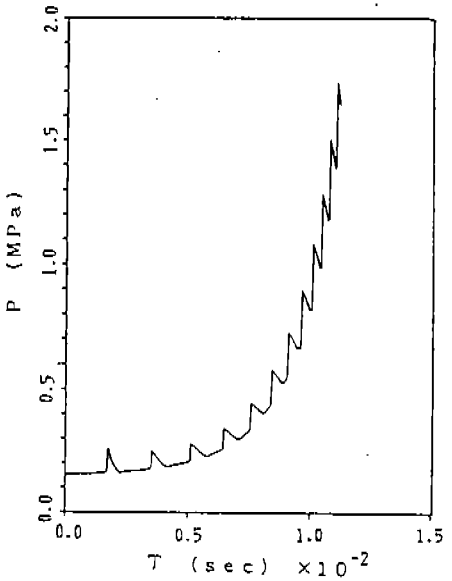

Fig.8 Result of calcuration about the pressure cylinder chamber

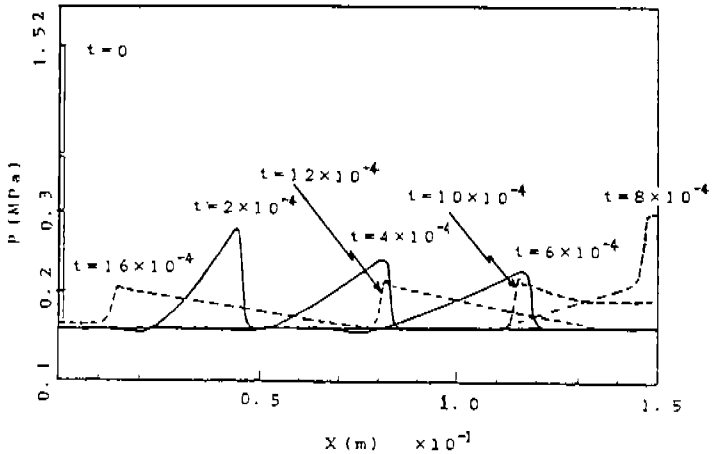

Fig.9 Result of calcuration about the shock wave propagation

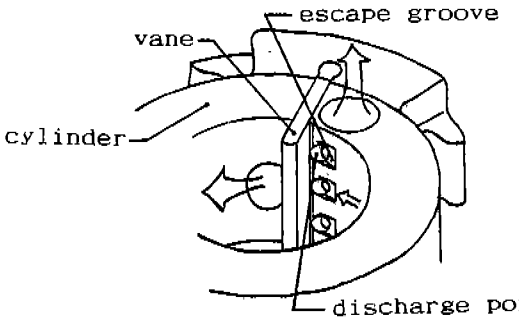

Fig.10 Oblique view of escape grooves

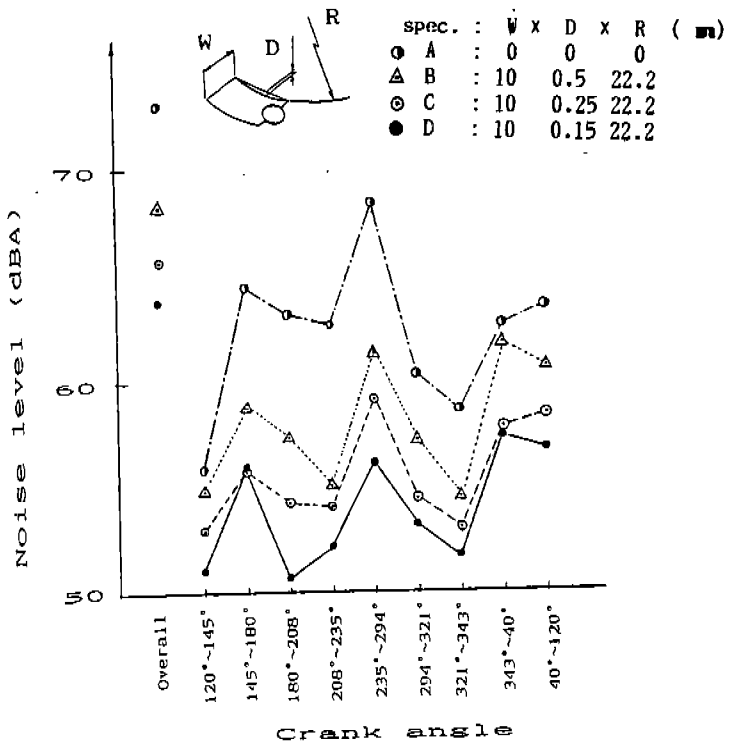

Fig.11 Noise level at each crank angle
in changing escape groove's dimension

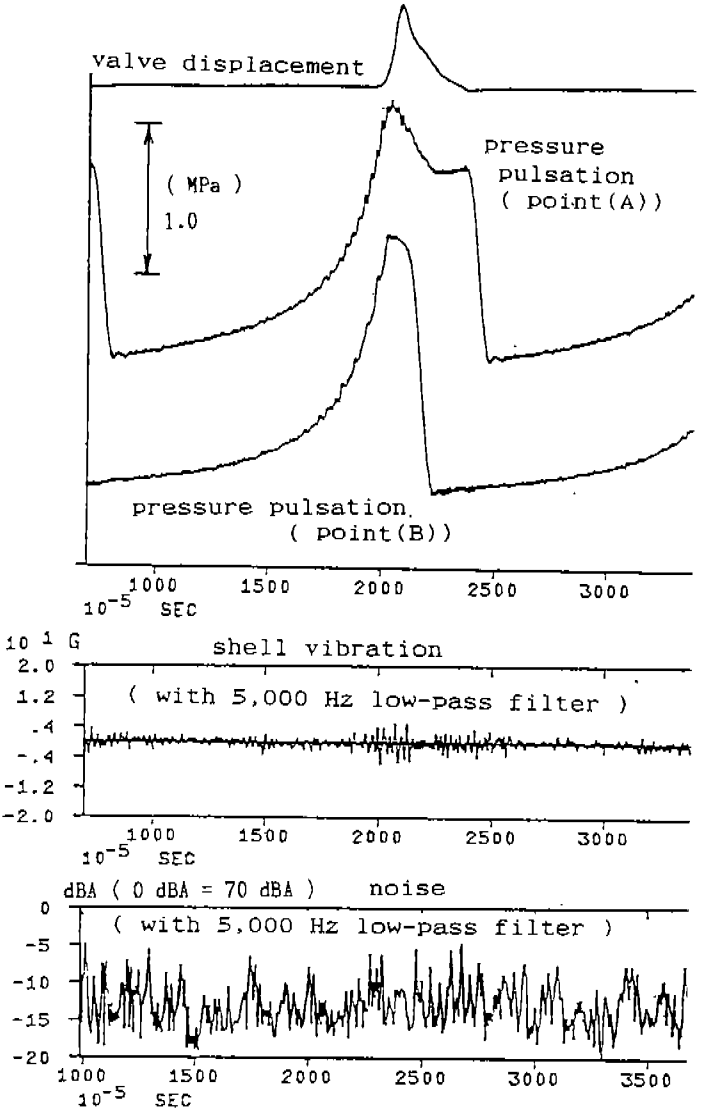

Fig.12 Test data of MODEL A'
on the A-3 condition

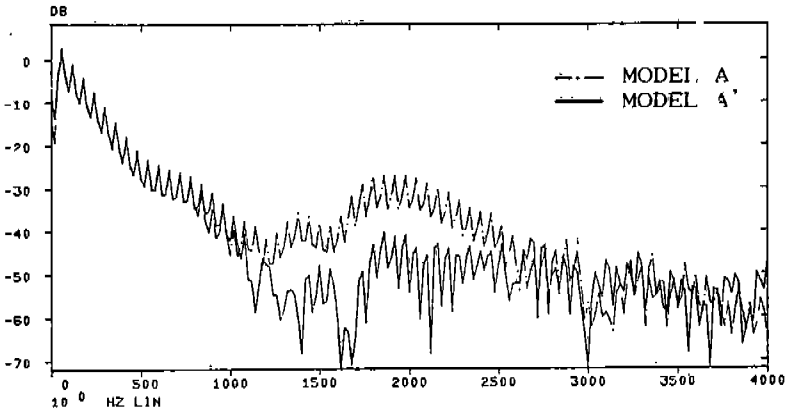

Fig.13 Pressure pulsation power spectra (point B) of MODEL A and MODEL A'

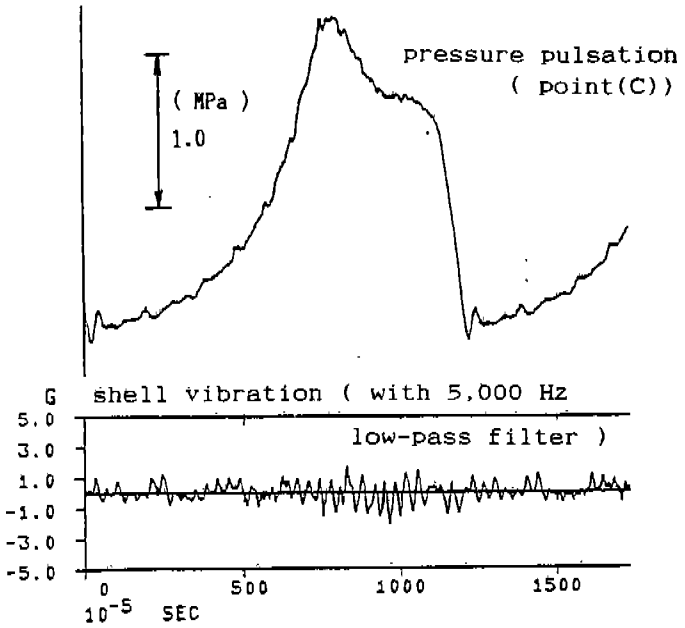

Fig.14 Test data of MODEL B' on the B-4 condition

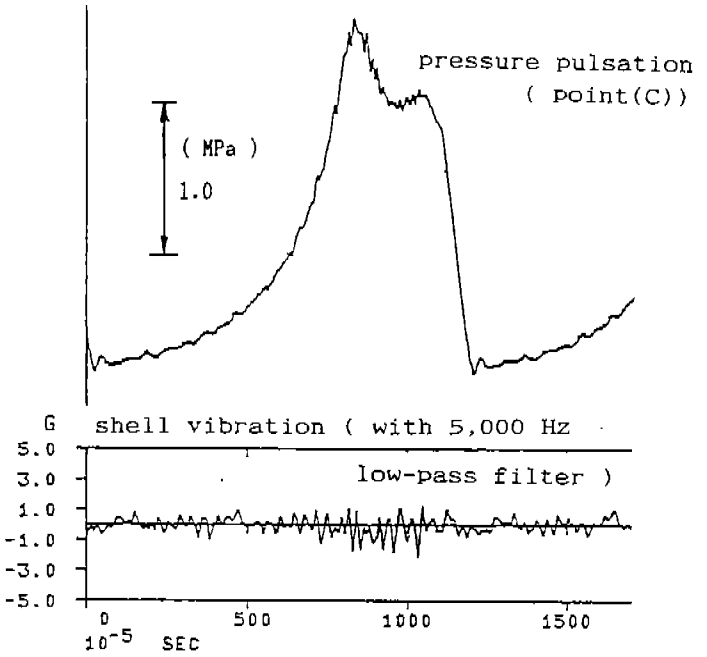

Fig.15 Test data of MODEL B' on the B-5 condition

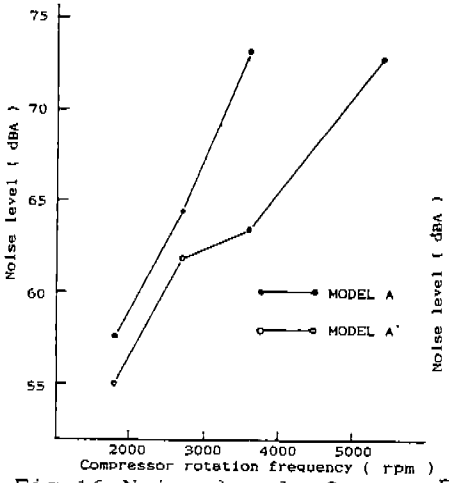

Fig.16 Noise level of MODEL A and MODEL A'

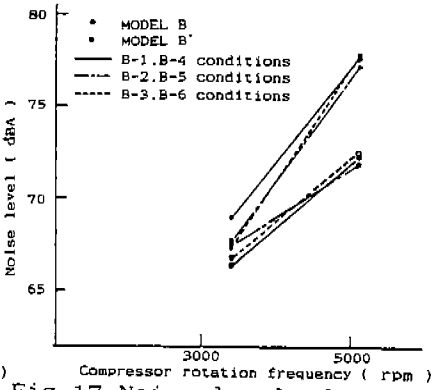

Fig.17 Noise level of MODEL B and MODEL B'